



HAL
open science

Improved Performance of YIG (Y₃Fe₅O₁₂) Films Grown on Pt-Buffered Si Substrates by Chemical Solution Deposition Technique

Xin Guo, Ying Chen, Genshui Wang, Jun Ge, Yuanyuan Zhang, Xiaodong Tang, Freddy Ponchel, Denis Remiens, Xianlin Dong

► **To cite this version:**

Xin Guo, Ying Chen, Genshui Wang, Jun Ge, Yuanyuan Zhang, et al.. Improved Performance of YIG (Y₃Fe₅O₁₂) Films Grown on Pt-Buffered Si Substrates by Chemical Solution Deposition Technique. Journal of the American Ceramic Society, 2016, 99 (7), pp.2217-2220. 10.1111/jace.14293 . hal-03525733

HAL Id: hal-03525733

<https://hal.science/hal-03525733v1>

Submitted on 3 Oct 2024

HAL is a multi-disciplinary open access archive for the deposit and dissemination of scientific research documents, whether they are published or not. The documents may come from teaching and research institutions in France or abroad, or from public or private research centers.

L'archive ouverte pluridisciplinaire **HAL**, est destinée au dépôt et à la diffusion de documents scientifiques de niveau recherche, publiés ou non, émanant des établissements d'enseignement et de recherche français ou étrangers, des laboratoires publics ou privés.

Improved Performance of YIG ($\text{Y}_3\text{Fe}_5\text{O}_{12}$) Films Grown on Pt-Buffered Si Substrates by Chemical Solution Deposition Technique

Xin Guo,[‡] Ying Chen,[‡] Genshui Wang,[‡] Jun Ge,[‡] Yuanyuan Zhang,[§] Xiaodong Tang,[§] Freddy Ponchel,[¶] Denis Remiens,[¶] and Xianlin Dong^{‡,†}

[‡] Key Laboratory of Inorganic Function Materials and Devices, Shanghai Institute of Ceramics, Chinese Academy of Sciences, University of Chinese Academy of Sciences, 1295 Dingxi Rd., Shanghai 200050, China

[§] Key Laboratory of Polar Materials and Devices, Ministry of Education, Department of Electronic Engineering, East China Normal University, 500 Dongchuan Rd., Shanghai 200241, China

[¶]Institute of Electronics, Microelectronics and Nanotechnology (IEMN)–DOAE, UMR CNRS 8520, Université des Sciences et Technologies de Lille, Villeneuve d'Ascq Cedex 59652, France

High-quality Yttrium iron garnet (YIG) films with crack-free surface and improved magnetic performance were grown on platinum (Pt)-buffered Si substrates by chemical solution deposition technique. The saturation magnetization of obtained YIG films can reach 124 emu/cm^3 , which was the 88% theoretical value of YIG single crystal. The effects of annealing condition were also discussed. When annealed at 750°C for 1 h, YIG films showed a very small coercive field of 12 Oe and the peak-to-peak ferromagnetic resonance linewidth can be as low as 95 Oe at 9.10 GHz. The results demonstrated that YIG films prepared on Pt-buffered Si substrates can be beneficial to the application of YIG films to integrated devices.

Keywords: yttrium/yttrium compounds; films; ferromagnetism/ferromagnetic materials; magnetic materials/properties

I. Introduction

YTRITIUM iron garnet (YIG) $\text{Y}_3\text{Fe}_5\text{O}_{12}$ has been one of the most studied garnet ferrites since its discovery.^{1,2} YIG is an important magnetic compound with many applications to microwave tunable devices, such as microwave generators and analyzers. YIG-based phase shifters and tuners are vital components in phased array radar systems.^{3–6} The applications are attributed to lower losses of YIG in microwave band, such as high resistivity,⁷ small magnetic uniaxial anisotropy,⁸ and extremely narrow ferromagnetic resonance (FMR) linewidth $\Delta H < 1 \text{ Oe}$.⁹

Normally, YIG films are grown on gadolinium gallium garnet $\text{Gd}_3\text{Ga}_5\text{O}_{12}$ (GGG) substrate which has the same crystal structure, similar thermal expansion coefficient (GGG: $9.3 \times 10^{-6}/^\circ\text{C}$, YIG: $9.2 \times 10^{-6}/^\circ\text{C}$) and good lattice match (GGG: $a = 12.376 \text{ \AA}$, YIG: $a = 12.380 \text{ \AA}$) with YIG. Up to now, epitaxial YIG films are only obtained on GGG substrates.^{10–13} However, the integration of YIG films to semiconductors such as Si, quartz, GaAs, Al_2O_3 , and so on are necessary for integrated devices application.^{14–17} Si-based substrates are widely used for the excellent integrated performance and large-scale production. However, because of the lattice mismatch and thermal expansion coefficient, the difference

between Si ($4.7 \times 10^{-6}/^\circ\text{C}$) and YIG ($9.2 \times 10^{-6}/^\circ\text{C}$),¹⁴ cracks always appear in films when prepared on Si. It is necessary to introduce a buffer layer on Si substrates to reduce interface mismatch. Some efforts have been made to avoid cracks, such as using oxidized Si or Si/CeO₂ substrates, but there is no significant improvement.^{13,14,18} Platinum (Pt) is mostly used as an electrode material for the perfect conductivity, few are focused on its compatibility. Pt has a thermal expansion coefficient of $9.0 \times 10^{-6}/^\circ\text{C}$, which is very close to YIG ($9.2 \times 10^{-6}/^\circ\text{C}$), for this reason that Pt maybe a good buffer layer to avoid YIG cracks when annealing. Therefore, we tried YIG preparation on Pt-buffered Si substrates for the purpose to obtain better performance.

Chemical solution deposition (CSD) technique was utilized to prepare YIG films. Compared with PLD and sputtering, some pores can be formed in YIG films with CSD method, which will leave space for reducing stress and lowering cracks formation. Furthermore, CSD technique can have large-scale production, excellent chemical homogeneity, and lower cost.

In this work, YIG thin films were deposited on Pt-buffered Si/SiO₂ substrates by CSD method, which showed good performances with crack-free and improved magnetic values. The effect of annealing conditions was also discussed.

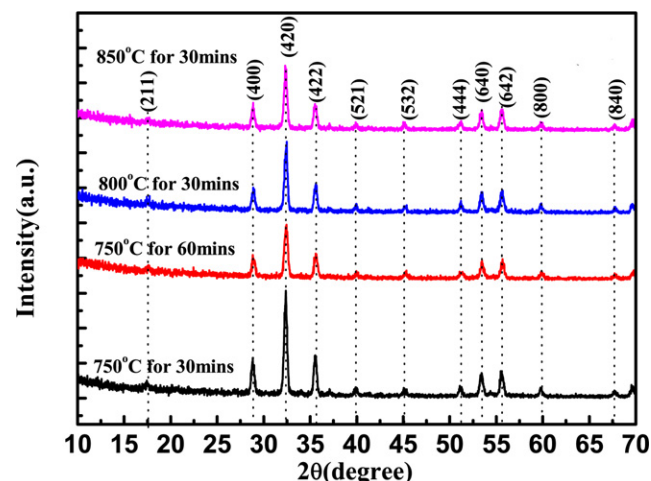


Fig. 1. XRD patterns of YIG films in four annealing conditions: (1) 750°C for 30 min, (2) 750°C for 60 min, (3) 800°C for 30 min, (4) 850°C for 30 min.

P. Gomez—contributing editor

[†]Author to whom correspondence should be addressed. e-mail: xldong@mail.sic.ac.cn

II. Experimental Procedure

YIG films were deposited on Pt/SiO₂/Si substrates by CSD method as follows: Yttrium oxide and ferric nitrate were firstly dissolved in acetic acid and deionized water with a concentration of 0.1 M/L, then the solution was deposited on Pt/SiO₂/Si substrates with a spinning speed of 5000 rpm for 30 s. After, the obtained gel coatings were dried at 200°C and then pyrolyzed at 400°C. At last, films were crystallized under four annealing conditions in air: (1) 750°C for 30 min, (2) 750°C for 60 min, (3) 800°C for 30 min, (4) 850°C for 30 min.

The structure and morphology of films were checked by X-ray diffraction with CuK₁ radiation (Model RAX-10; Rigaku, Tokyo, Japan) and atomic force microscopy, AFM (Bruker, Karlsruhe, Germany). An impedance analyzer Agilent 4294A (Agilent Technology Japan, Ltd., Kobe-shi, Japan) was employed to show the dielectric properties. The hysteresis loops (M-H) were obtained in a vibrating sample

magnetometer of PPMS (PPMS-9, Quantum Design, San Diego, CA). The room FMR was carried out using an electron spin resonance (JEOL-FA, Tokyo, Japan) spectrometer working at 9.10 GHz.

III. Results and Discussions

XRD patterns of YIG films are shown in Fig. 1 with different annealing conditions: (1) 750°C for 30 min, (2) 750°C for 60 min, (3) 800°C for 30 min, (4) 850°C for 30 min. As shown, pure poly-crystallization YIG garnet structures can be formed without any second phase. From calculation, the lattice constants of YIG films were about 1.2372 nm, which were much closer to the bulk YIG value (1.2380 nm). It meant that YIG films on Pt/Si substrate can maintain good garnet structure with a small strain, for the reason that Pt can buffer the lattice constant mismatch between YIG and Si substrates.

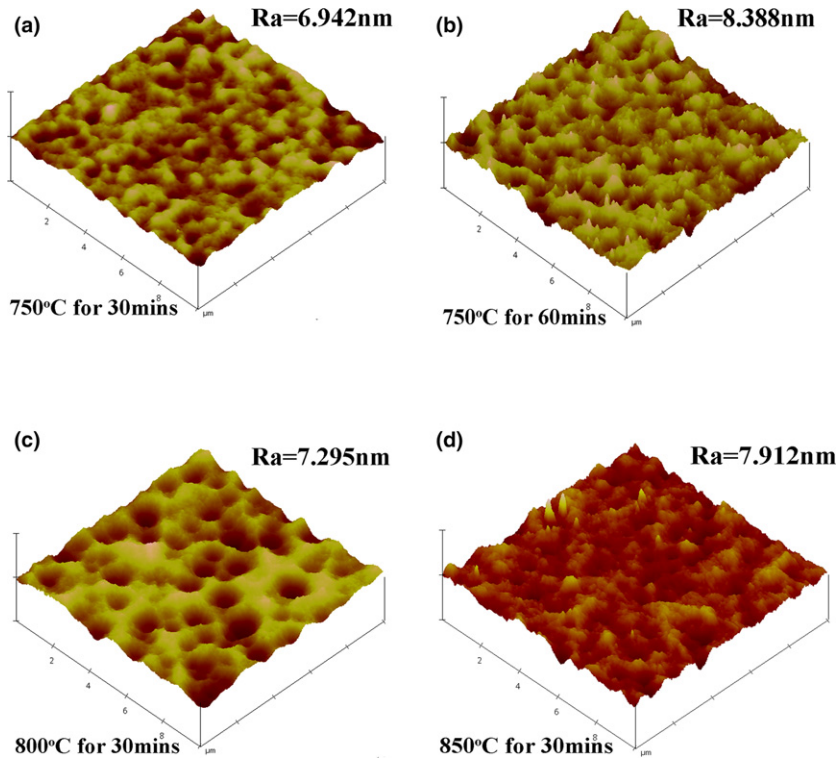


Fig. 2. 3D AFM images of YIG films crystallized in (a) 750°C for 30 min, (b) 750°C for 60 min, (c) 800°C for 30 min, (d) 850°C for 30 min.

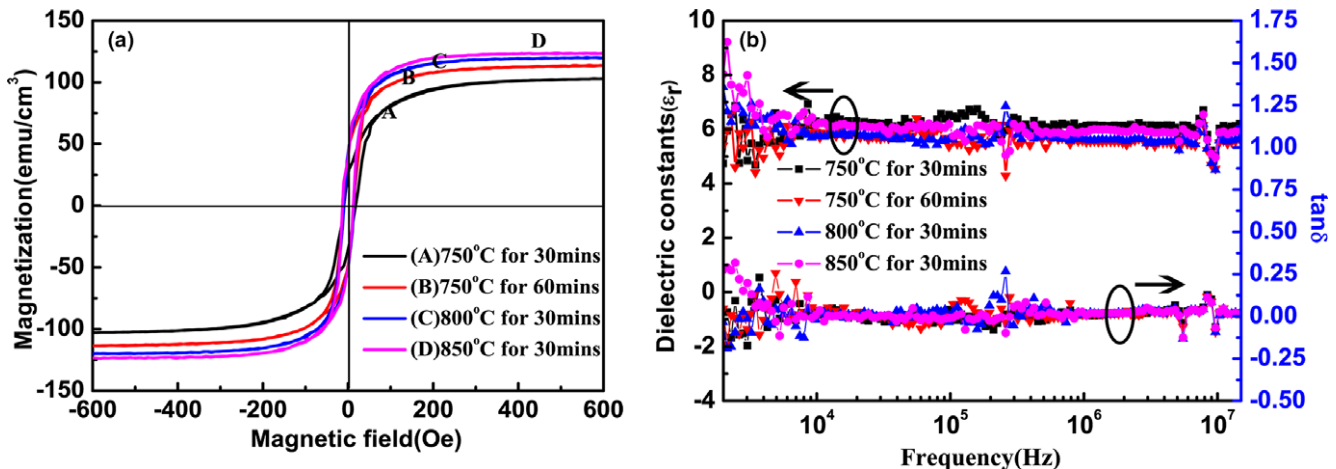


Fig. 3. Magnetic and dielectric properties of YIG films in different annealing conditions: (A) 750°C for 30 min, (B) 750°C for 60 min, (C) 800°C for 30 min, (D) 850°C for 30 min. (a) M-H loops of YIG films. The coercive field (H_c), saturation magnetization (M_s and $4\pi M_s$) can be read from curves and are shown in Table I. (b) Dielectric constants and dielectric loss ($\tan\delta$) of YIG films upon frequency at room temperature.

The surface morphology was displayed by AFM with an area of $10\ \mu\text{m}\times 10\ \mu\text{m}$ in Fig. 2. No cracks can be seen on the surface, which was excellent performance compared with other reports of cracks.^{16,19} Pt has a thermal expansion of $9.0\times 10^{-6}/^\circ\text{C}$, which is much closer to YIG ($9.2\times 10^{-6}/^\circ\text{C}$), in this condition, when YIG grown on Pt-buffered Si substrate, there was little thermal strain in films, resulting in better surface without cracks. Film roughness was lower than 10 nm, with increasing annealing time and temperature, RMS was increased, which comes from the high energy for grain growth when higher temperature and longer time.

Figure 3 and Table I gave the magnetic and dielectric properties of YIG films: (A) 750°C for 30 min, (B) 750°C for 60 min, (C) 800°C for 30 min, (D) 850°C for 30 min. As shown in Fig. 3(a), all films showed typically soft

Table I. Magnetic Data of YIG Films in Different Annealing Conditions

Annealing conditions	Magnetic performance		
	Hc (Oe)	Ms (emu/cm ³)	4πMs(G)
750°C for 30 min	14	103	1293
750°C for 60 min	13	110	1382
800°C for 30 min	12	120	1507
850°C for 30 min	12	124	1552

ferromagnetism with narrow loops. The dependence of saturation magnetization (Ms) and coercive field (Hc) on annealing conditions are shown in Table I. With increasing annealing temperature and time, Ms was increased for better crystallization. In 850°C for 30 min, Ms was 124 emu/cm³, resulting a magnetic induction $4\pi\text{Ms}$ of 1.55 kG, which can reach the 88% value of single-crystal YIG ($4\pi\text{Ms} = 1.75\ \text{kG}$). The little decrease in saturation magnetization maybe due to the interface between YIG and substrate, which would reduce the effective density of YIG films. Furthermore, the strain-induced anisotropy in polycrystalline YIG films could lower magnetization.¹⁹ The magnetic value we got was close to the (111) orientation YIG films prepared by PLD on GGG with Hc = 3.8 Oe and $4\pi\text{Ms} = 1.58\ \text{kG}$.²⁰ The average coercive field of YIG films was about 13 Oe, which was much smaller than YIG films deposited on Si, Si/CeO₂, or porous SiO₂ substrates.^{14,15,19,21}

The frequency dependence of YIG films permittivity are shown in Fig. 3(b). The dielectric constants and losses were almost independent of frequency, showing stable values in a broad frequency from 10 kHz to 20 MHz. As shown, the dielectric constants were kept at 6–8 and the dielectric loss of $\tan\delta$ can be as low as 0.008@20 MHz. Though the test frequency was much lower than microwave range, the results were still significant because it showed the better stability and lower losses of YIG films, which could be the proof of CSD technique feasibility to prepare YIG films on Si.

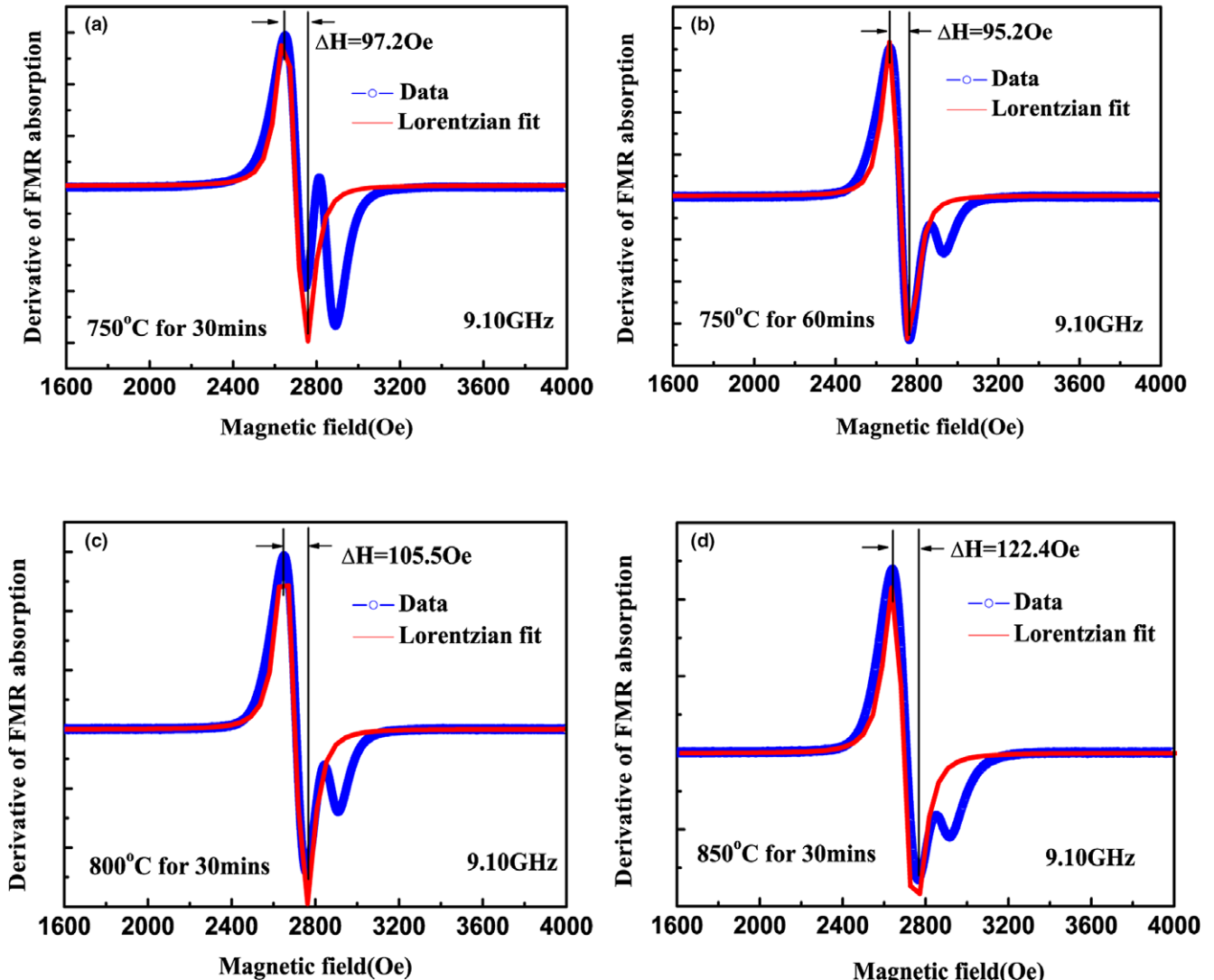


Fig. 4. FMR curves at 9.10 GHz of YIG films in: (a) 750°C for 30 min, (b) 750°C for 60 min, (c) 800°C for 30 min, (d) 850°C for 30 min.

Table II. Comparison of YIG Films Grown on Pt/SiO₂/Si in this Work with Those Reported in Literatures

Samples Method	YIG/Pt/SiO ₂ /Si(100) CSD (Chemical solution deposition)	YIG/SiO ₂ /Si(100) ¹³ Sputtering	YIG/Sapphire ¹⁵ Aerosol deposition	YIG/Quartz ¹⁹ PLD	YIG/Porous Silicon ²⁵ PLD
Annealing temperature	750°C	900°C	1280°C	750°C	650°C
Coercive field (Oe)	13	16	6	25	30
Peak-to-peak FMR width (Oe)	95	150	198	200	96

In Fig. 4, FMR curves and linewidth ΔH_{FMR} were shown in different annealing conditions. All curves showed a good Lorentzian fit (red line). A second peak appeared besides the main resonance absorption, which was also reported in others' work.^{13,21,22} According to G. Woltersdorf and Vladimir L. Safonov's theory,^{23,24} this behavior can be attributed to defects in films. The confluence process can occur in the presence of defects, impurities, or fluctuations which can induce an additional absorption. The measured linewidth versus frequency is often interpreted with a simple relationship:²³

$$\Delta H_{\text{FMR}(f)} = \Delta H(0) + \alpha \frac{2\pi f}{\gamma} \quad (1)$$

where f is the radio-frequency, α is the Gilbert damping constants ($\alpha = (10.3 \pm 0.5) \times 10^{-4}$), γ ($=2.8$ MHz/Oe) is the gyromagnetic ratio, and $\Delta H(0)$ is the linewidth at zero frequency. $\Delta H(0)$ is a long-range inhomogeneity-caused line broadening, which is extrinsic and depends on the film quality. The narrower ΔH , the better is the crystal quality and lower losses. The lowest FMR width was obtained with $\Delta H = 95.2$ Oe at 9.10 GHz when annealed at 750°C for 60 min in air, which was smaller than films on other nongarnet substrates.^{13,15,19,25} The comparisons of specific values are shown in Table II. We can see clearly that YIG films in this work showed a smaller coercive field ($H_c = 13$ Oe) and lower resonance width ($\Delta H = 95.2$ Oe) with 750°C annealing. The data suggested that YIG prepared on Pt-buffered Si/SiO₂ substrate by CSD can show an improved performance including the surface quality and magnetic property with a relative lower annealing temperature. Our results proved that Pt can successfully buffer the lattice structure mismatch and large thermal expansion difference between YIG and Si as predicted, improving the performance of YIG films with less cracks and defects.

IV. Conclusions

In summary, this work showed high-quality YIG films growth on Pt-buffered Si substrates. Films with crack-free and improved magnetic performance were obtained, showing a small coercive field ($H_c = 13$ Oe) and low FMR width ($\Delta H = 95$ Oe). Furthermore, we proved the feasibility of CSD technique for YIG films on Si substrates with a relative low annealing temperature. This is an important proof that high-quality YIG films can be fabricated on Si-based substrate when introducing Pt as a buffer layer. It would be a promising way for better application of YIG films to silicon integrated devices with lower loss.

Acknowledgments

This work was supported by the National Natural Science Foundation of China (Nos. 61371059 and 51302295), Shanghai Natural Science Foundation (No. 13ZR1445600), the Visiting Scholar Foundation of Key Lab. of Micro-nano Devices and System Technology in Chongqing University, and international partnership project of Chinese Academy of Science.

References

¹F. Bertaut and F. FORRAT, "The Structure of Ferrimagnetism Rare Earth Ferrites," *Compt. Rend.*, **242**, 382 (1956).

²S. Geller and M. Gilleo, "Structure and Ferrimagnetism of Yttrium and Rare-Earth-Iron Garnets," *Acta. Cryst.*, **10**, 239 (1957).

³G.-M. Yang, J. Wu, J. Lou, M. Liu, and N. X. Sun, "Low-Loss Magnetically Tunable Bandpass Filters With YIG Films," *IEEE Trans. Magn.*, **49**, 5063–8 (2013).

⁴Y. Zhu, G. Qiu, and C. S. Tsai, "A Magnetically- and Electrically-Tunable Microwave Phase Shifter Using Yttrium Iron Garnet/Gadolinium Gallium Garnet Thin Film," *J. Appl. Phys.*, **111**, 07A5021–3 (2012).

⁵K. Bi, W. Zhu, M. Lei, and J. Zhou, "Magnetically Tunable Wideband Microwave Filter Using Ferrite-Based Metamaterials," *Appl. Phys. Lett.*, **106**, 1735071–4 (2015).

⁶D. Matatagui, O. V. Kolokoltsev, N. Qureshi, E. V. Mejía-Uriarte, and J. M. Saniger, "A Novel Ultra-High Frequency Humidity Sensor Based on a Magnetostatic Spin Wave Oscillator," *Sens. Actuat. B Chem.*, **210**, 297–301 (2015).

⁷D. C. Bullock, "Negative Resistance, Conductive Switching, and Memory Effect in Silicon-Doped Yttrium-Iron Garnet Crystals," *Appl. Phys. Lett.*, **17**, 199–201 (1970).

⁸Ü. Özgür, Y. Alivov, and H. Morkoç, "Microwave Ferrites, Part 1: Fundamental Properties," *J. Mater. Sci.: Mater. Electron.*, **20**, 789–834 (2009).

⁹J. Das, Y.-Y. Song, N. Mo, P. Krivosik, and C. E. Patton, "Electric-Field-Tunable Low Loss Multiferroic Ferrimagnetic-Ferroelectric Heterostructures," *Adv. Mater.*, **21**, 2045–9 (2009).

¹⁰Y. Sun, Y.-Y. Song, H. Chang, M. Kabatek, M. Jantz, et al., "Growth and Ferromagnetic Resonance Properties of Nanometer-Thick Yttrium Iron Garnet Films," *Appl. Phys. Lett.*, **101**, 1524051–5 (2012).

¹¹T. Liu, H. Chang, V. Vlaminck, Y. Sun, M. Kabatek, et al., "Ferromagnetic Resonance of Sputtered Yttrium Iron Garnet Nanometer Films," *J. Appl. Phys.*, **115**, 17A5011–3 (2014).

¹²M. Haidar, M. Ranjbar, M. Balinsky, R. K. Dumas, S. Khartsev, and J. Åkerman, "Thickness- and Temperature-Dependent Magnetodynamic Properties of Yttrium Iron Garnet Thin Films," *J. Appl. Phys.*, **117**, 17D1191–4 (2015).

¹³Y.-M. Kang, S.-H. Wee, S.-I. Baik, S.-G. Min, S.-C. Yu, et al., "Magnetic Properties of YIG (Y₃Fe₅O₁₂) Thin Films Prepared by the Post Annealing of Amorphous Films Deposited by rf-Magnetron Sputtering," *J. Appl. Phys.*, **97**, 10A3191–3 (2005).

¹⁴Q. H. Yang, H. W. Zhang, Q. Y. Wen, and Y. L. Liu, "Effects of off-Stoichiometry and Density on the Magnetic and Magneto-Optical Properties of Yttrium Iron Garnet Films by Magnetron Sputtering Method," *J. Appl. Phys.*, **108**, 0739011–5 (2010).

¹⁵S. D. Johnson, E. R. Glaser, S.-F. Cheng, F. J. Kub, and C. R. Eddy, "Characterization of as-Deposited and Sintered Yttrium Iron Garnet Thick Films Formed by Aerosol Deposition," *Appl. Phys. Exp.*, **7**, 0355011–4 (2014).

¹⁶A. Siblini, I. Khalil, J. P. Chatelon, M. F. Blanc-Mignon, D. Jamon, and J. J. Rousseau, "Influence of Annealing in Vacuum and in Air on Magnetic, Crystallographic and Morphological Properties of Thin YIG Films," *Jems 2012 - Joint Eur. Magnetic Symp.*, **40**, 160041–4 (2012).

¹⁷Q. H. Yang, H. W. Zhang, Q. Y. Wen, Y. L. Liu, and J. Q. Xiao, "Tuning Magnetic Properties of Yttrium Iron Garnet Film With Oxygen Partial Pressure in Sputtering and Annealing Process," *J. Appl. Phys.*, **105**, 07A5011–3 (2009).

¹⁸T. Goto, Y. Eto, K. Kobayashi, Y. Haga, M. Inoue, and C. A. Ross, "Vacuum Annealed Cerium-Substituted Yttrium Iron Garnet Films on non-Garnet Substrates for Integrated Optical Circuits," *J. Appl. Phys.*, **113**, 17A9391–13 (2013).

¹⁹S. Katlakunta, and S. R. Murthy, "Effect of Oxygen Pressure on Structural and Magnetic Properties of YIG Thin Films," *AIP Conf. Proc.*, **719**, 719–20 (2012).

²⁰Y. Sun, Y.-Y. Song, and M. Wu, "Growth and Ferromagnetic Resonance of Yttrium Iron Garnet Thin Films on Metals," *Appl. Phys. Lett.*, **101**, 0824051–3 (2012).

²¹E. Popova, N. Keller, F. Gendron, M. Guyot, M. C. Brianso, et al., "Structure and Magnetic Properties of Yttrium-Iron-Garnet Thin Films Prepared by Laser Deposition," *J. Appl. Phys.*, **90**, 1422–8 (2001).

²²E. Popova, N. Keller, F. Jomard, L. Thomas, M. C. Brianso, et al., "Exchange Coupling in Ultrathin Epitaxial Yttrium Iron Garnet Film," *Eur. Phys. J. B*, **31**, 69–74 (2003).

²³G. Woltersdorf, "Spin Pumping and two-Magnon Scattering in Magnetic Multilayers," Ph.D. thesis, Simon Fraser University, 2004.

²⁴V. L. Safonov, and H. N. Bertram, "Linear Stochastic Magnetization Dynamics and Microscopic Relaxation Mechanisms," *J. Appl. Phys.*, **94**, 529–538 (2003).

²⁵H. Zheng, J. J. Zhou, J. X. Deng, P. Zheng, L. Zheng, et al., "Preparation of two-Dimensional Yttrium Iron Garnet Magnonic Crystal on Porous Silicon Substrate," *Mater. Lett.*, **123**, 181–3 (2014). □